Separation of Rare-Earth and Transition-Metal Contributions to the Interfacial Dzyaloshinskii-Moriya Interaction in Ferrimagnetic Co-Gd Alloys

Zhiyuan Zhao,[1,2] Dan Su,[3] Tao Lin,[3] Zhicheng Xie,[1,2] Duo Zhao,[1,2] Jianhua Zhao,[1,2] Na Lei,[3,*] and Dahai Wei[1,2,†]

[1] *State Key Laboratory of Superlattices and Microstructures, Institute of Semiconductors, Chinese Academy of Sciences, Beijing 100083, China*

[2] *Center of Materials Science and Optoelectronics Engineering, University of Chinese Academy of Sciences, Beijing 100190, China*

[3] *Fert Beijing Institute, MIIT Key Laboratory of Spintronics, School of Integrated Circuit Science and Engineering, Beihang University, Beijing 100191, China*

(Received 12 December 2022; revised 27 February 2023; accepted 20 March 2023; published 13 April 2023)

Ferrimagnetic materials composed of rare earth (RE) and transition metals (TM) are of great interest for spintronic devices due to their tunable net moments and magnetic transport behaviors. Here we experimentally study the Dzyaloshinskii-Moriya interaction (DMI) in Co-Gd ferrimagnets and find that the DMI strength increases substantially as the temperature approaches its moment compensation point. By subtracting the contribution of Heisenberg exchange coupled Co-Co moments mediated by Pt from the total DMI strength, we observe a relationship $D_{\mathrm{Co-Gd}} \sim M_s^{0.2\pm0.06}$. The lower order indicates the weaker Heisenberg exchange compared with Co-Co moments in Co-Gd alloys. Our results reveal the intrinsic physics of DMI in RE-TM alloys by separating the different contributions of TM-TM and RE-TM sublattice moments from the total DMI and show the promising prospect for the fabrication of skyrmions in RE-TM ferrimagnets near the compensation point.

DOI: 10.1103/PhysRevApplied.19.044037

I. INTRODUCTION

Rare-earth and transition-metal (RE-TM) ferrimagnetic (FIM) alloys, such as Co-Tb [1], Co-Gd [2–5], and Gd-Fe-Co [6], possess a strong negative exchange interaction and tunable net magnetization. Because of the competition between magnetic moments of the RE and TM sublattices, the net magnetization of RE-TM alloys can be tuned by either temperature or composition. Thus, there could be critical points where the magnetization or angular momentum is fully compensated. Previous work has experimentally realized 10-nm small-size skyrmions near the compensation point in Pt/Gd-Co/Ta [7] and reduced skyrmion Hall angle in Pt/Gd-Fe-Co/MgO heterostructures [8], indicating the suppression of skyrmion Hall effect in RE-TM alloys. The interfacial Dzyaloshinskii-Moriya interaction (DMI) in the heavy metal (HM) and FIM heterostructures is crucial to the stabilization of the skyrmions [9,10] and chiral Neél domain walls [11,12], and attract the attention both theoretically [13] and experimentally [14].

The interfacial DMI in the conventional HM/ferromagnetic heterostructures has been intensively explored, and the correlation between the DMI strength (D) and saturation magnetization M_s is revealed [15–18]. By using the Green function theory and correcting the single-ion anisotropy in the system, one expects the $D \propto M_s^2$ [15]. Zhou *et al*. observed $D \propto M_s^{1.86\pm0.16}$ in Pt/CoFeB, which is similar to the scaling of exchange stiffness [16]; while $D \propto M_s^{4.9\pm0.7}$ in $[\mathrm{Pt/Co/Cu}]_{15}$ [17] and $D \propto M_s^{5.25\pm0.3}$ in Pt/Co [18] were also reported experimentally. Despite the controversy, the scaling of D as a function of M_s gives a viable route to analyze the DMI in HM/FM [18]. However, the scaling of D versus M_s in HM/FIM bilayers is barely explored. Rahul Mishra *et al*. presented the D of Co-Gd alloys with different compositions [2] without any further analysis. The systematical study of the D in HM/FIM bilayers, especially near its compensation, would lead to a proper and deeper understanding of the interfacial DMI in a RE-TM ferrimagnet.

In this study, we perform measurements of effective DMI strength in Pt/Co-Gd alloys as the temperature approaches the compensation. The electric transport measurements are performed to extract the DMI effective fields (H_{DMI}) at different temperatures. The effective DMI strength acquired with $D^* = \mu_0 \Delta H_{\mathrm{DMI}} M_s$ reveals an increasing behavior as the temperature approaches the compensation point. By considering the additive DMI Co-Co and Co-Gd moments with Pt at the interface, the correlation $D_{\mathrm{Co-Gd}} \propto M_s^{0.2\pm0.06}$, is observed. These results

*na.lei@buaa.edu.cn
†dhwei@semi.ac.cn

reveal the intrinsic physics of the increasing D with the temperature in Pt/Co-Gd heterostructures by separating the different contributions of Co-Co and Co-Gd–Co-Gd sublattice moments to the total DMI and show encouraging prospects in the application of ferrimagnetic skyrmion-based spintronics devices.

II. SAMPLE PREPARATION AND CHARACTERIZATION

As shown by the inset in Fig. 1(a), the stack of Ta buffer(2)/Pt(3)/$Co_{1-x}Gd_x$(4.6)/Al(6.7) are deposited on thermally oxidized Si substrates by using magnetron sputtering with a base pressure of 5×10^{-8} Torr, all thicknesses are in nm. The 4.6-nm $Co_{1-x}Gd_x$ amorphous alloys are co-sputtered with the Co and Gd targets. The chemical composition of $Co_{1-x}Gd_x$ alloy is $Co_{0.7}Gd_{0.3}$, which is calculated from the precalibrated deposition rates versus the sputtering power and further confirmed by the energy-dispersive x-ray spectroscopy measurements (see the Supplemental Material [19]). The bottom Ta and the top Al acts as the buffer and capping layers, respectively. The film stack is patterned into Hall cross devices with a width of 15 μm by using photolithography and ion milling, and the schematic illustrations of the device and transport measurement setup are shown in Fig. 1(a). Note that long-range order is not expected for the sputtered Co-Gd alloy via the measurement of high-resolution transmission electron microscopy (see the Supplemental Material [20]). The morphology of the deposited film has also been measured via atomic force microscopy with a root-mean-square roughness of 0.97 nm (see the Supplemental Material [21]).

Measurements of anomalous Hall effect (AHE) are performed to characterize the magnetic properties. Typical hysteresis loops of the anomalous Hall resistance (R_{AH}) for the sample are shown in Fig. 1(b), the perpendicular magnetic anisotropy can be achieved at all temperatures from 160 to 300 K. The positive R_{AH} can be clearly seen at temperatures above 238 K indicating Co dominance in the net magnetization; while the negative R_{AH} appears at temperatures below 227 K as Gd dominant. The R_{AH} changes sign across the critical temperature of magnetization compensation (T_M), while the moments of the Co sublattice reverse between the Co- and Gd-dominant cases. Similar results are obtained in previous works, showing that the anomalous Hall effect is derived from the spin-dependent scattering of the TM sublattice [22].

The coercivity field (H_C) significantly increases up to 2 kOe as the temperatures approach T_M, due to the smaller and net magnetization M_s [23]. The M_s versus temperature measured by a superconducting quantum interference device with a 2-kOe out-of-plane field applied, is shown in Fig. 1(c). The T_M of the stack can be precisely determined as the minimum of M_s at 233 K, indicated by the vertical dashed line.

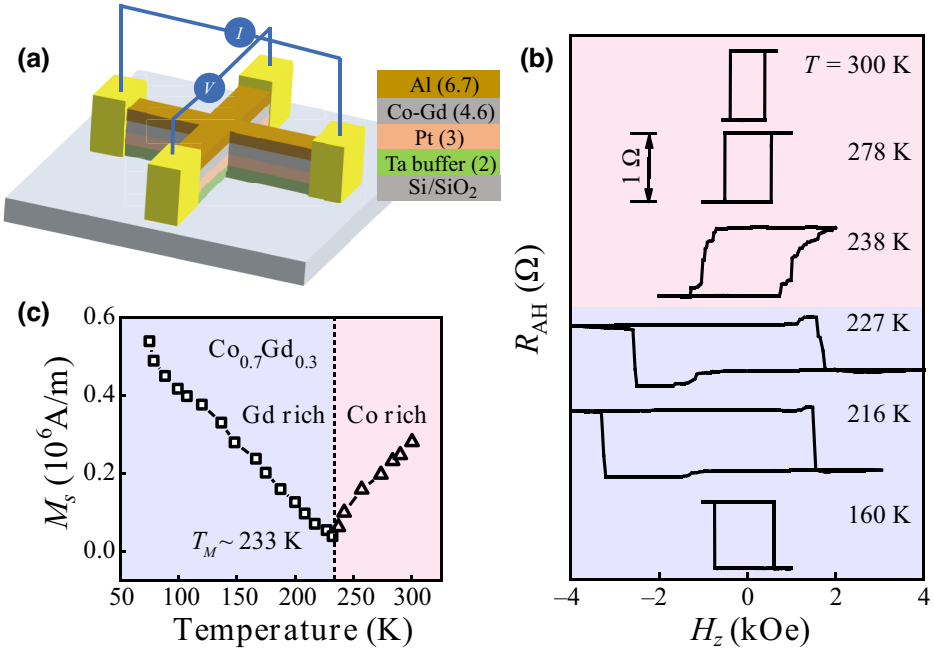

FIG. 1. (a) Schematic illustrations of the sample structure and transport measurement setup on a Hall-bar device. (b) The anomalous Hall resistance of the stack with $Co_{0.7}Gd_{0.3}$ at different temperatures. (c) The net magnetization plotted with the temperature of the stack with an out-of-plane field of 2 kOe, confirms that the T_M of the stack is around 233 K.

III. RESULTS AND DISCUSSION

We then perform the measurement of the Dzyaloshinskii-Moriya interaction effective field (H_{DMI}) by using the method reported by Kim *et al.* in 2017 [24]. For a magnetic droplet with perpendicular magnetic anisotropy, the nucleation field (H_n) versus the in-plane field (H_x) exhibits a threshold, which reveals the effect of DMI. As depicted in the inset figure of Fig. 2(b), the AHE is measured with the external magnetic field (H_{ex}) applied at different angles θ with respect to the z axis. Figure 2(a) shows the representative anomalous Hall resistance switching from down to up at 160 K with a series of different θ. The switching fields (H_{sw}) are extracted from AHE hysteresis loops for each θ and plotted in Fig. 2(b), which are fitted well with $H_{\mathrm{sw}} = H_C(\theta = 0)/\cos\theta$ for small angles ($0^\circ < \theta < 60^\circ$) as the red solid line. The bubble domain expands under an out-of-plane magnetic field, which enables us to extract H_{DMI} through the expansion of the domain according to the Kondorsky model [25]. However, for larger θ the fitting is invalid since the domain-wall propagation is derived from the magnetic droplet model, as indicated by the dashed red line in Fig. 2(b). Switching of magnetization under H_{sw} implies the process of the reversed-domain nucleation and the domain-wall propagation. Therefore, the z component $H_n = H_{\mathrm{sw}}\cos\theta$ acts as the nucleation field, while the x component $H_x = H_{\mathrm{sw}}\sin\theta$ acts as the in-plane field. Figures 2(c) and 2(d) show the measured H_n with respect to H_x at various temperatures above and below the T_M, respectively. The tendency of H_n with respect to H_x is consistent with results reported elsewhere [6], and H_{DMI} is extracted as the threshold value of H_x marked by the black arrows at each temperature. The detailed results at other temperatures (see the Supplemental Material [26]).

As shown by the top panel in Fig. 3(a), H_{DMI} gradually increases as the temperature approaches the compensation point. It is difficult to accurately extract the H_{DMI} near the compensation temperatures from 160 to 278 K when the ferrimagnet is close to its compensation. As shown in Fig. 1(b), the serrated AHE loops from 216 to 273 K are due to the formation of multidomains as competition between demagnetization energy and domain-wall energy in the temperature range near T_M [27]. As a result, the mechanism of domain-wall motion no longer fits the bubble-domain expansion, and Kim's method is not available. Samples with different Gd compensations are prepared and H_{DMI} increases with the Gd compensation, which is consistent with the temperature dependence of H_{DMI} (see the Supplemental Material [28]).

Then we focus on the behavior of effective DMI strength (D^*) at different temperatures. The effective DMI strength is given by $D^* = \mu_0 \Delta H_{\mathrm{DMI}} M_s$, where μ_0 is the vacuum permeability, $\mathbf{\Delta} = \sqrt{A/K_{\mathrm{eff}}}$ is the domain width, and A is the exchange stiffness constant [29]. $K_{\mathrm{eff}} = H_K M_s/2$

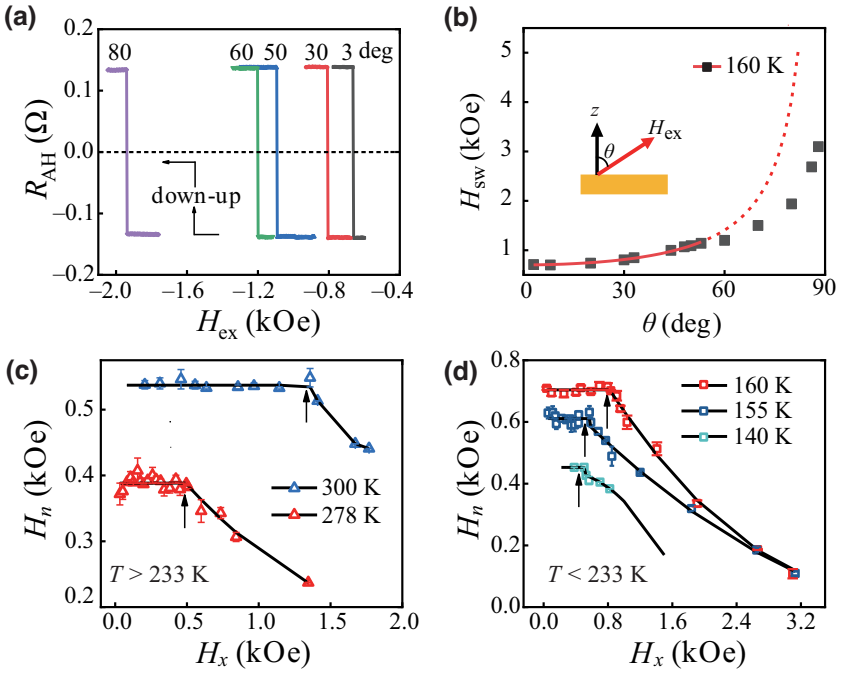

FIG. 2. (a) The anomalous Hall resistance of the stack under different angles θ at 160. (b) H_{sw} plots with respect to the angle θ at 160 K. The red line is the fitting curve of $H_{\mathrm{sw}} = H_C(\theta = 0)/\cos\theta$, according to the Kondorsky model. The in-plane field is applied at different angles θ, with respect to the z axis, as shown in the inset of (b). (c),(d) The nucleation field as a function of the in-plane field extracted from angle-dependent AHE loops of the stack at various temperatures above (c) and below (d) the T_M, respectively. The black arrows denote the value of H_{DMI}.

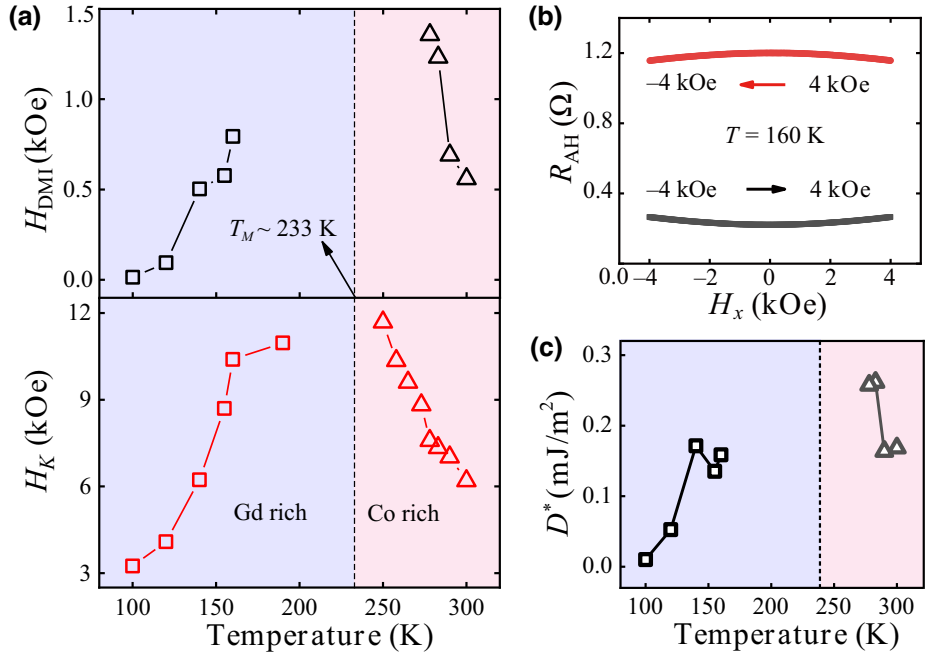

FIG. 3. (a) H_{DMI} and H_K plotted with the temperature of the stack. (b) The anomalous Hall resistance of the stack is measured with the in-plane magnetic field at 160 K, which is used to extract the effective anisotropy field H_K. (c) The DMI strength D^* increases as the temperature approach its compensation point T_M.

is the effective perpendicular magnetic anisotropy energy density [30]. H_K is extracted from R_{AH} measured with the in-plane field shown in Fig. 3(b) and plotted in the bottom panel of Fig. 3(a). D^* is calculated with the measured H_K, M_s, and A, taken as $A(T) \propto M_s^{1.8}$ [15,31] with 1×10^{-11} J/m at 300 K [2]. Note that the demagnetization effect has been included in the K_{eff} of the magnetic thin film. As depicted in Fig. 3(c), we observe that the effective DMI strength of Pt/Co-Gd heterostructure (D^*) increases as the temperature approaches its compensation point.

It has been reported that in the HM/FM heterostructures, DMI strength is proportional to $M_s^{4.9\pm0.7}$ in $[\mathrm{Pt/Co/Cu}]_{15}$ thin-film heterostructures [17], $M_s^{5.25\pm0.3}$ in Pt/Co bilayers [18], where the higher order indicating DMI is more sensitive to thermal fluctuations than bulk magnetic properties [18] and $M_s^{1.86\pm0.16}$ in a multilayer of Ta/Pt/Co-Fe-B/Ru/Pt/Co-Fe-B/Ru/Pt, in which the exchange stiffness constant is manipulated by the Ru space layer [16].

However, the intrinsic physics of DMI in HM/FIM heterostructure has rarely been investigated. As shown in Fig. 4(b), the effective DMI strength D^* decreases with the net magnetization of Co-Gd alloy and fitted with $D^*(T) \propto M_s^{-2.3\pm0.1}$, the negative power exponent is different from that of HM/FM heterostructures, in which DMI shares the same physics with the Heisenberg exchange as temperature changes [15,16]. As the result, the intrinsic mechanism of the effective DMI strength in Co-Gd alloy cannot be simply analyzed by the relationship between D^* and net magnetization. Previous work has shown that in Co-Gd alloys, the Heisenberg exchange integral J of Co-Co is 12.7 times larger than Co-Gd, meanwhile, J of RE-TM is 4.4 times larger than Gd-Gd [32], which indicates that ferromagnetically coupled Co-Co sublattice moments and antiferromagnetically coupled Co-Gd sublattice moments are co-existed in Co-Gd alloys, as shown in Fig. 4(a). Co-Co (Co-Gd) moments are parallelly (antiparallelly) coupled first because of large Heisenberg exchange interaction strength then interact with Pt. In order to analyze the intrinsic DMI of the magnetic heterostructures, the three-site model is widely utilized in previous studies [33,34]. Further, Kent *et al*. have taken both the Co-Co bond and Co-Gd bond in their calculation process of DMI in the Pt/Gd-Co/X (X = Ta, W, Ir) material system [35]. However, previous work suggests that DMI in the bulk-symmetry broken Fe-Gd alloy is not expected [36], and compared with 5*d* metal Pt, SOC from the 4*f* rare-earth Gd cannot establish DMI, therefore, the role of SOC induced by Gd to generate DMI is not expected. As a result, moments located on the sublattices in RE-TM alloy mediated by the Pt atom in a Fert-Levy triangle are taken into consideration. According to the Fert-Levy model [37], three-site triangles of $\mathrm{Pt-Co-Co}$ and $\mathrm{Pt-Co-Gd}$ contribute to the total DMI strength by neglecting the contribution of $\mathrm{Pt-Gd-Gd}$ due to its weak interaction [32,37,38]. The total DMI strength can be calculated by

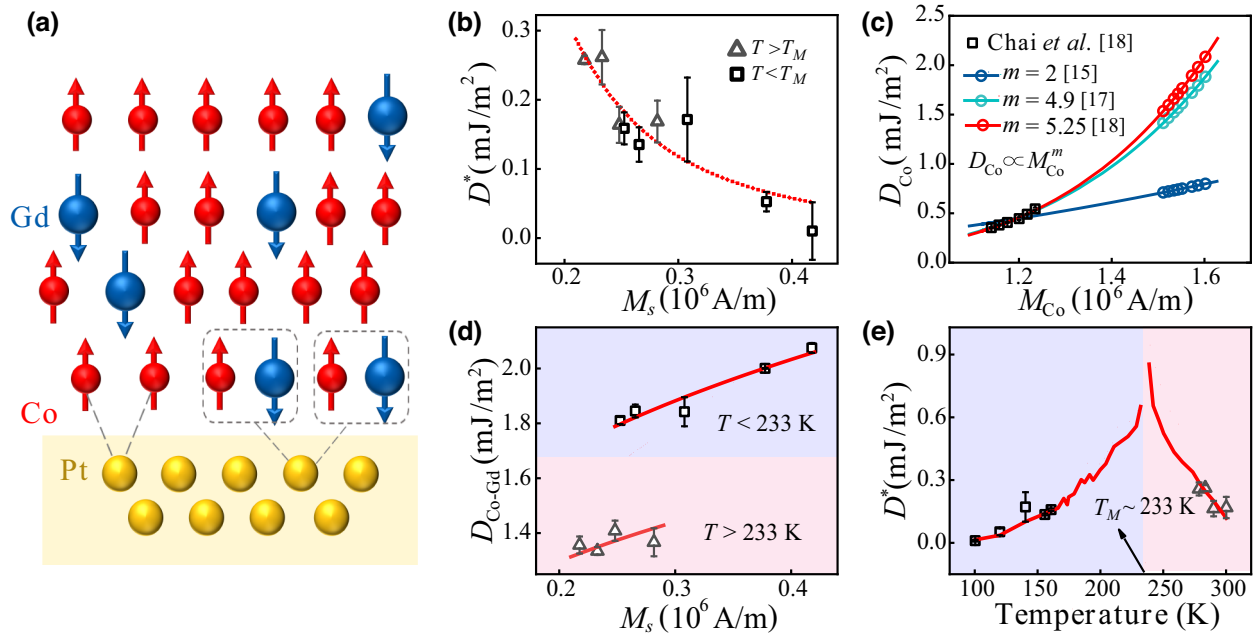

FIG. 4. (a) Illustration of sublattice moments and the Fert-Levy triangles in Co-Gd alloy. (b) The effective DMI strength D^* plots with the saturation magnetization M_s of Co-Gd alloy and indicates a negative correlation. (c) D_{Co} versus M_{Co} extracted from Chai *et al.* [18] (open squares, left) are fitted with $D_{Co} \propto M_{Co}^m$, where $m = 2$ [15], 4.9 [17], and 5.25 [18], respectively. Open circles on the right are D_{Co} plotted with the nominal magnetization of Co in the $Co_{0.7}Gd_{0.3}$ alloy at different temperatures, with $m = 2$ [15], 4.9 [17], and 5.25 [18] respectively. (d) $D_{Co\text{-}Gd}$ subtracted from $D^* = \xi_{Pt\text{-}Co} M_{Co}^{5.25} + D_{Co\text{-}Gd}$ plotted with M_s and fitted with $D_{Co\text{-}Gd} \propto M_s^m$above and below T_M, respectively. (e) The effective DMI strength (D^*) is plotted with temperature and fitted with $D(T) = \xi_{Pt\text{-}Co} M_{Co}^{5.25}(T) + \xi_{Pt\text{-}Co\text{-}Gd} M_s^{0.26}(T)$. The fitting line reveals an increasing behavior as temperature approach T_M.

the following formula [37]:

$$D = \sum_l D_{ijl}(R_{l,i}, R_{l,j}, R_{i,j}). \tag{1}$$

To simplify, the DMI strength can be depicted as $D(T) = \alpha_1 D_{Co}(T) + \alpha_2 D_{Co\text{-}Gd}(T)$ in Co-Gd alloy where α_1 and α_2 are parameters that describe the proportion of the two Heisenberg exchanged magnetic moments in the DMI of Co-Gd alloy.

Due to difficulties in separating the magnetization of Co in the Co-Gd alloy, we calculate the nominal Co thickness in our $Co_{0.7}Gd_{0.3}$ is approximately 2.3 nm from the precalibrated deposition rates and evaluate M_{Co} as 1.512×10^6 A/m at 300 K. M_{Co} is plotted with $M_{Co} = M_{Co}(0)(1 - (T/T_C)^{2.06})$, here the deviation of 2.06 from the expected Bloch $T^{3/2}$ law is attributed to the granular nature of sputtered films [39]. Chai *et al.* [18] have reported $D_{Co}(T) \propto M_{Co}^{5.25}$ in Pt/Co bilayer and have been extracted as shown in open squares of Fig. 4(c). By fitting the data with different order m in the $D_{Co}(T) \propto M_{Co}^m$, which have been reported previously, we acquire D_{Co} as a function of M_{Co} for our system, $Pt/Co_{0.7}Gd_{0.3}$ heterostructure, at different temperatures from 100 to 300 K with $m = 2$ [15], 4.9 [17], and 5.25 [18], respectively, as shown in open circles of Fig. 4(c).

The value of $D_{Co\text{-}Gd}$ is given by subtracting D_{Co} from the D^*. For each m, we find positive correlations with the parameter n between $D_{Co\text{-}Gd}$ and net magnetic moments, $D_{Co\text{-}Gd}(T) \propto M_s^n$ as shown in Table I. In comparison with $m = 2$, which is calculated with mean-field approximation theoretically [15], the higher order, 4.9 and 5.25, are related to the localized magnetic moment in the Pt layer and the 3*d*-5*d* orbital interactions at the interface [17,40] reveal more about the two-dimensional nature of the HM/FM interface than three-dimensional magnetic properties [18]. Pt/Co-Gd in this work is similar to the material system of Pt/Co used in Chai *et al.* [18], thus, we find the fit for $m = 5.25$ and $D_{Co\text{-}Gd} \sim M_s^{0.2\pm0.06}$.

As Nembach *et al.* have suggested, DMI and Heisenberg exchange interaction share the same physics [41], and the corresponding expression for the exchange stiffness constant $A_{ij} \propto D_{ij} M/(2g)$ (where M is the total magnetic

TABLE I. The extracted parameter n from $D_{Co\text{-}Gd}(T) \propto M_s^n$ for each m in the $D_{Co}(T) \propto M_{Co}^m$, respectively.

m	n ($T > 233$ K)	n ($T < 233$ K)
2 [15]	0.1 ± 0.06	0.1 ± 0.09
4.9 [17]	0.2 ± 0.07	0.2 ± 0.07
5.25 [18]	0.2 ± 0.06	0.2 ± 0.06

moment and g is the Landé factor) has been derived by Liechtenstein *et al*. [42] with the theory of nonrelativistic multiple scattering. We suggest that compared with the higher-power component observed in HM/FM heterostructures, the lower component, for instance, $n = 0.2 \pm 0.06$ for the $D_{\mathrm{Co\,-\,Gd}}(T) \propto M_s^n$ extracted from $m = 5.25$, is derived from the weaker Heisenberg interaction of Co-Gd sublattice moments compared with ferromagnetically coupled Co-Co moments.

The calculated DMI strength is defined as $D(T) = \xi_{\mathrm{Pt\,-\,Co}} M_{\mathrm{Co}}^{5.25}(T) + \xi_{\mathrm{Pt\,-\,Co\,-\,Gd}} M_s^{0.26}(T)$, where the parameters $\xi_{\mathrm{Pt\,-\,Co\,-\,Co}}$ and $\xi_{\mathrm{Pt\,-\,Co\,-\,Gd}}$ are extracted from Figs. 4(c) and 4(d). As shown in Fig. 4(e), the effective D^* is fitted with the $D(T)$ as a function of the temperature. An increasing behavior of $D(T)$ versus temperature is observed near T_M, indicating that in the HM/FIM interface, both the ferromagnetically coupled TM-TM sublattice moments and antiferromagnetically coupled RETM-RETM sublattice moments contribute to the total DMI strength.

IV. SUMMARY

In conclusion, we experimentally study the effective DMI strength with temperature in ferrimagnet Co-Gd alloys. The H_{DMI} increases as the temperature approaches its magnetization compensation temperature. D^* increases as the temperature approach T_M and the relationship $D^*(T) \propto M_s^{-2.3\pm0.1}$ is observed. Further, by considering the contribution of Fert-Levy triangles of $\mathrm{Pt-Co-Co}$ and $\mathrm{Pt-Co-Gd}$ to the D^*, $D_{\mathrm{Co-Gd}}$ is subtracted from the D^* and reveals a positive correlation with the net magnetization of Co-Gd. The fit for $D_{\mathrm{Co\,-\,Gd}}(T) \propto M_s^{0.2\pm0.06}$ is observed. The smaller power component is attributed to the weaker Heisenberg exchange of Co-Gd sublattice moments compared with Co-Co. The calculated DMI strength D defined as $D(T) = \xi_{\mathrm{Pt\,-\,Co}} M_{\mathrm{Co}}^{5.25}(T) + \xi_{\mathrm{Pt\,-\,Co\,-\,Gd}} M_s^{0.2}(T)$ is increasing as temperature approaches compensation, which is consistent with D^*. Despite the limitations of the measurement based on the magnetic droplet nucleation model, the methods including static domain spacing analysis and Brillouin light scattering could be candidates to investigate the DMI strength near T_M. Our results raise questions about the specific contribution of the temperature dependence of DMI in Pt/Co-Gd alloy, the relation of DMI to the exchange constant for the RE-TM and TM-TM sublattice moments in HM/FIM bilayers, respectively, and the modulation of DMI by changing the contribution rate of TM-TM and RE-TM in ferrimagnetic alloys with different compensations. Owing to the strong temperature dependence of DMI, the stabilization of small-size skyrmions near the compensation point is excepted, which is encouraging for device applications.

ACKNOWLEDGMENTS

This work is supported by the National Natural Science Foundation of China (Grants No. 52061135105, No. 12074025, and No. 11834013), the CAS Project for Yong Scientists in Basic Research (Grant No. YSBR-030), and the Key Research Project of Frontier Science of Chinese Academy of Sciences (Grants No. XDB44000000 and No. XDB28000000).

[1] R. Q. Zhang, *et al.*, Current-induced magnetization switching in a CoTb amorphous single layer, Phys. Rev. B **101**, 214418 (2020).

[2] Rahul Mishra, Jiawei Yu, Xuepeng Qiu, M. Motapothula, T. Venkatesan, and Hyunsoo Yang, Anomalous Current-Induced Spin Torques in Ferrimagnets Near Compensation, Phys. Rev. Lett. **118**, 167201 (2017).

[3] Ting Fu, Shuangfeng Li, Xiaoyu Feng, Yongwei Cui, Jiguang Yao, Bo Wang, Jiangwei Cao, Zhong Shi, Desheng Xue, and Xiaolong Fan, Complex anomalous Hall effect of CoGd alloy near the magnetization compensation temperature, Phys. Rev. B. **103**, 064432 (2021).

[4] M. Binder, A. Weber, O. Mosendz, G. Woltersdorf, M. Izquierdo, I. Neudecker, J. R. Dahn, T. D. Hatchard, J.-U. Thiele, C. H. Back, and M. R. Scheinfein, Magnetization dynamics of the ferrimagnet CoGd near the compensation of magnetization and angular momentum, Phys. Rev. B. **74**, 134404 (2006).

[5] Y. Quessab, J.-W. Xu, C. T. Ma, W. Zhou, G. A. Riley, J. M. Shaw, H. T. Nembach, S. J. Poon, and A. D. Kent, Tuning interfacial Dzyaloshinskii-Moriya interactions in thin amorphous ferrimagnetic alloys, Sci. Rep. **10**, 7447 (2020).

[6] Duck-Ho Kim, *et al.*, Bulk Dzyaloshinskii–Moriya interaction in amorphous ferrimagnetic alloys, Nat. Mater. **18**, 685 (2019).

[7] Lucas Caretta, Maxwell Mann, Felix Büttner, Kohei Ueda, Bastian Pfau, Christian M. Günther, Piet Hessing, Alexandra Churikova, Christopher Klose, Michael Schneider, Dieter Engel, Colin Marcus, David Bono, Kai Bagschik, Stefan Eisebitt, and Geoffrey S. D. Beach, Fast current-driven domain walls and small skyrmions in a compensated ferrimagnet, Nat. Nanotechnol. **13**, 1154 (2018).

[8] Seonghoon Woo, Kyung Mee Song, Xichao Zhang, Yan Zhou, Motohiko Ezawa, Xiaoxi Liu, S. Finizio, J. Raabe, Nyun Jong Lee, Sang-Il Kim, Seung-Young Park, Younghak Kim, and Jae-Young Kim, Dongjoon Lee1, OukJae Lee, Jun Woo Choi, Byoung-Chul Min, Hyun Cheol Koo & Joonyeon Chang, Current-driven dynamics and inhibition of the skyrmion Hall effect of ferrimagnetic skyrmions in GdFeCo films, Nat. Commun. **9**, 959 (2018).

[9] J. Sampaio, V. Cros, S. Rohart, A. Thiaville, and A. Fert, Nucleation, stability and current-induced motion of isolated magnetic skyrmions in nanostructures, Nat. Nanotechnol. **8**, 839 (2013).

[10] Wanjun Jiang, Pramey Upadhyaya, Wei Zhang, Guoqiang Yu, M. Benjamin Jungfleisch, Frank Y. Fradin, John E. Pearson, Yaroslav Tserkovnyak, Kang L. Wang, Olle Heinonen, Suzanne G. E. te Velthuis, and Axel Hoffmann,

Blowing magnetic skyrmion bubbles, Science **349**, 283 (2015).
[11] P. P. J. Haazen, E. Muré, J. H. Franken, R. Lavrijsen, H. J. M. Swagten, and B. Koopmans, Domain wall depinning governed by the spin Hall effect, Nat. Mater. **12**, 299 (2013).
[12] Jacob Torrejon, Junyeon Kim, Jaivardhan Sinha, Seiji Mitani, Masamitsu Hayashi, Michihiko Yamanouchi, and Hideo Ohno, Interface control of the magnetic chirality in CoFeB/MgO heterostructures with heavy metal underlayer, Nat. Commun. **5**, 4655 (2014).
[13] Carla Quispe Flores, Alexandra R. Stuart, Kristen S. Buchanan, and Karen L. Livesey, Analytic calculation for the stray field above Néel and Bloch magnetic domain walls in a rectangular nanoribbon, J. Magn. Magn. Mater. **513**, 167164 (2020).
[14] Zhaochu Luo, Aleš Hrabec, Trong Phuong Dao, Giacomo Sala, Simone Finizio, Junxiao Feng, Sina Mayr, Jörg Raabe, Pietro Gambardella, and Laura J. Heyderman, Current-driven magnetic domain-wall logic, Nature **579**, 214 (2020).
[15] Levente Rózsa, Unai Atxitia, and Ulrich Nowak, Temperature scaling of the Dzyaloshinsky-Moriya interaction in the spin wave spectrum, Phys. Rev. B **96**, 094436 (2017).
[16] Yifan Zhou, Rhodri Mansell, Sergio Valencia, Florian Kronast, and Sebastiaan van Dijken, Temperature dependence of the Dzyaloshinskii-Moriya interaction in ultrathin films, Phys. Rev. B **101**, 054433 (2020).
[17] Sarah Schlotter, Parnika Agrawal, and Geoffrey S. D. Beach, Temperature dependence of the Dzyaloshinskii-Moriya interaction in Pt/Co/Cu thin film heterostructures, Appl. Phys. Lett. **113**, 092402 (2018).
[18] Yabing Zhang, Xiangjie Kong, Guofu Xu, Ying Jin, Changjun Jiang, and Guozhi Chai, Direct observation of the temperature dependence of the Dzyaloshinskii–Moriya interaction, J. Phys. D: Appl. Phys. **55**, 195304 (2022).
[19] See the Supplemental Material at http://link.aps.org/supplemental/10.1103/PhysRevApplied.19.044037 for measured energy-dispersive x-ray spectroscopy of CoGd alloy to confirm its composition.
[20] See the Supplemental Material at http://link.aps.org/supplemental/10.1103/PhysRevApplied.19.044037 for the HRTEM image of previously prepared multilayers.
[21] See the Supplemental Material at http://link.aps.org/supplemental/10.1103/PhysRevApplied.19.044037 for the atomic force microscopy image of the oxidized Si substrate and Pt/CoGd/Al thin film.
[22] Niklas Roschewsky, Tomoya Matsumura, Suraj Cheema, Frances Hellman, Takeshi Kato, Satoshi Iwata, and Sayeef Salahuddin, Spin-orbit torques in ferrimagnetic GdFeCo alloys, Appl. Phys. Lett. **109**, 112403 (2016).
[23] Yaohan Xu, Dongdong Chen, Shucheng Tong, Huanjian Chen, Xuepeng Qiu, Dahai Wei, and Jianhua Zhao, Spin Polarization Compensation in Ferrimagnetic $Co_{1-x}Tb_x$/Pt Bilayers Revealed by Spin Hall Magnetoresistance, Phys. Rev. Appl. **14**, 034064 (2020).
[24] Sanghoon Kim, Peong-Hwa Jang, Duck-Ho Kim, Mio Ishibashi, Takuya Taniguchi, Takahiro Moriyama, Kab-Jin Kim, Kyung-Jin Lee, and Teruo Ono, Magnetic droplet nucleation with a homochiral Néel domain wall, Phys. Rev. B **95**, 220402(R) (2017).
[25] Kevin R. Coffey, Thomas Thomson, and Jan-Ulrich Thiele, Angular dependence of the switching field of thin-film longitudinal and perpendicular magnetic recording media, J. Appl. Phys. **15**, 4553 (2002).
[26] See the Supplemental Material at http://link.aps.org/supplemental/10.1103/PhysRevApplied.19.044037 for the measurements of H_{DMI} at other temperatures.
[27] M. V. Logunov, S. S. Safonov, A. S. Fedorov, A. A. Danilova, N. V. Moiseev, A. R. Safin, S. A. Nikitov, and A. Kirilyuk, Domain Wall Motion Across Magnetic and Spin Compensation Points in Magnetic Garnets, Phys. Rev. Appl. **15**, 064024 (2021).
[28] See the Supplemental Material at http://link.aps.org/supplemental/10.1103/PhysRevApplied.19.044037 for relationships between H_{DMI} and Gd-composition of Co-Gd alloys.
[29] Chi-Feng Pai, Maxwell Mann, Aik Jun Tan, and Geoffrey S. D. Beach, Determination of spin torque efficiencies in heterostructures with perpendicular magnetic anisotropy, Phys. Rev. B **93**, 144409 (2016).
[30] M. T. Johnson, P. J. H. Bloemen, F. J. A. den Broeder, and J. J. de Vries, Magnetic anisotropy in metallic multilayers, Rep. Prog. Phys. **59**, 1409 (1996).
[31] U. Atxitia, D. Hinzke, O. Chubykalo-Fesenko, U. Nowak, H. Kachkachi, O. N. Mryasov, R. F. Evans, and R. W. Chantrell, Multiscale modeling of magnetic materials: Temperature dependence of the exchange stiffness, Phys. Rev. B **82**, 134440 (2010).
[32] Masud Mansuripur and M. F. Ruane, Mean-field analysis of amorphous rare earth-transition metal alloys for thermomagnetic recording, IEEE Trans. Magn. **22**, **33** (1986).
[33] C. Moreau-Luchaire, C. Motafis, N. Reyren, J. Sampaio, C. A. F. Vaz, N. Van Horne, K. Bouzehouane, K. Garcia, C. Deranlot, P. Warnicke, P. Wohlhüter, J.-M. George, M. Weigand, J. Raabe, V. Cros, and A. Fert, Additive interfacial chiral interaction in multilayers for stabilization of small individual skyrmions at room temperature, Nat. Nanotechnol. **11**, 44 (2016).
[34] Wenqing He, Caihua Wan, Cuixiu Zheng, Yizhan Wang, Xiao Wang, Tianyi Ma, Yuqiang Wang, Chenyang Guo, Xuming Luo, Maksim E. Stebliy, Guoqiang Yu, Yaowen Liu, Alexey V. Ognev, Alexander S. Samardak, and Xiufeng Han, Field-free spin−orbit torque switching enabled by the interlayer Dzyaloshinskii−Moriya interaction, Nano Lett. **22**, 6857 (2022).
[35] Md Golam Morshed, Khoong Hong Khoo, Yassine Quessab, Jun-Wen Xu, Robert Laskowski, Prasanna V. Balachandran, Andrew D. Kent, and Avik W. Ghosh, Tuning Dzyaloshinskii-Moriya interaction in ferrimagnetic GdCo: A first-principles approach, Phys. Rev. B **103**, 174414 (2021).
[36] Qihan Zhang, Jinghua Liang, Le Zhao Kaiqi Bi, He Bai, Qirui Cui, Heng-An Zhou, Hao Bai, Hongmei Feng, Wenjie Song, Guozhi Chai, O. Gladii, H. Schultheiss, Tao Zhu, Junwei Zhang, Yong Peng, Hongxin Yang, and Wanjun Jiang, Quantifying the Dzyaloshinskii-Moriya Interaction

Induced by the Bulk Magnetic Asymmetry, Phys. Rev. Lett. **128**, 167202 (2022).

[37] Peter M. Levy and A. Fert, Anisotropy induced by nonmagnetic impurities in Cu Mn spin-glass alloys, Phys. Rev. B **23**, 4667 (1981).

[38] Dongdong Chen, Yaohan Xu, Shucheng Tong, Wenhui Zheng, Yiming Sun, Jun Lu, Na Lei, Dahai Wei, and Jianhua Zhao, Noncollinear spin state and unusual magnetoresistance in ferrimagnet Co-Gd, Phys. Rev. Mater. **6**, 014402 (2022).

[39] P. V. Hendriksen, S. Linderoth, and P. A. Lindgard, Finite-size modifications of the magnetic properties of clusters, Phys. Rev. B **48**, 7259 (1993).

[40] Jingzhi Fang, Huading Song, Bo Li, Ziqi Zhou, Juehan Yang, Benchuan Lin, Zhimin Liao, and Zhongming Wei, Large unsaturated magnetoresistance of 2D magnetic semiconductor Fe-SnS2 homojunction, J. Semicond. **43**, 092501 (2022).

[41] Hans T. Nembach, Justin M. Shaw, Mathias Weiler, Emilie Jué, and Thomas J. Silva, Linear relation between Heisenberg exchange and interfacial Dzyaloshinskii–Moriya interaction in metal films, Nat. Phys. **11**, 825 (2015).

[42] A. I. Liechtenstein, M. I. Katsnelson, and V. A. Gubanov, Local spin density functional approach to the theory of exchange interactions in ferromagnetic metals and alloys, J. Phys. F: Met. Phys. **14**, L125 (1984).